Nonlin. Processes Geophys. Discuss., 1, 977–997, 2014
www.nonlin-processes-geophys-discuss.net/1/977/2014/
doi:10.5194/npgd-1-977-2014

Nonlinear Processes in Geophysics
Discussions
Open Access

On the possibility of precursors of earthquakes in VLF range observed by DEMETER Satellite

D. K. Sondhiya[1], S. Kumar[2], and A. K. Gwal[1]

[1]Space Science Laboratory, Department of Physics, Barkatullah University, Bhopal-462026, India
[2]School of Engineering and Physics, The University of the South Pacific, Suva, Fiji

Received: 27 March 2014 – Accepted: 24 April 2014 – Published: 19 May 2014

Correspondence to: D. K. Sondhiya (deepsondhiya@gmail.com)

Published by Copernicus Publications on behalf of the European Geosciences Union & American Geophysical Union.

Abstract

Very Low Frequency (VLF) disturbances in the ionospheric electric field observed by DEMETER satellite prior to three different earthquakes that occurred during the years 2008–2009 have been presented. The electromagnetic wave data has been analyzed for few days before the earthquake with special attention to the variation in spectral characteristics and non-linear effects using the statistical and wavelet based techniques. Results indicate that the earthquake preparation process may disturb the ionospheric plasma and these disturbances can reach the non-linear stage leading to the strong variations in the electromagnetic field and plasma parameters. The enhancement in statistical parameters shows the coherent structure and intermittent phenomenon which is the signature of turbulence. The characteristics features of VLF disturbances have further been studied using the wavelet and bispectral analysis tools which provide useful information on the plasma turbulence.

1 Introduction

Over the seismic regions observations of anomalous plasma changes and electromagnetic emissions related with ionosphere indicate the existence of severe processes which control the state of circumterrestrial plasma for periods from several hours to several days (Boskova et al., 1994; He et al., 2009; Zhao et al., 2008). During the incidence of any strong earthquake, electric field may be generated within the upper atmosphere due to seismo-ionospheric coupling (Hayakawa, 1999; Hayakawa et al., 2004; Pulinets et al., 2004). Underground gas discharges carry submicron aerosols with them which influence near Earth's conductivity and generate extraneous electric field. Satellite observations show the presence of seismo-electromagnetic emissions in the frequency ranging from Ultra Low Frequency (ULF) to Very Low Frequency (VLF) in the seismically active zones prior to the commencement of any large earthquake (Fuzinawa and Takahashi, 1995; Karakelian et al., 2000; Nagao et al., 2002).

NPGD
1, 977–997, 2014

The influence of dynamic processes in the lower atmosphere and on the ionosphere was substantiated by satellite observations of electric field perturbations and plasma density fluctuations above earthquake development regions (Sorokin, 2007; Sorokin and Hayakawa, 2013). The mechanisms that could perturb the ionospheric plasma during the preparation of earthquakes are related to the redistribution of charges at the surface of the Earth, the emission of radioactive gas (radon) and the upward propagation of acoustic gravity waves (e.g. Pulinets and Boyarchuk, 2004, and references therein). The disturbances in the ionospheric plasma can reach the nonlinear stage leading to the phenomena of intermittence, which is considered as a sign of turbulence. Kinney et al. (1995) investigated the phenomenon of magneto-hydrodynamic turbulence using numerical simulations and found that influence of the coherent magnetic vortices is responsible for this behavior. The intermittence is characterized by the shape of the power spectrum and the high-order spectral analysis (McComb, 1990; Frisch, 1995). Hussain (1983) defined the Coherent Structures (CS) in turbulent variables (velocity, momentum, density, temperature, transport of mass and heat) that have high self-correlation. These structures are strongly associated with energy dissipation of the turbulent flows and are also a source of non-linearity at least in some scales.

The present paper deals with the analysis of phenomenon of intermittent and coherent structure in the ionospheric plasma in VLF range registered by DEMETER (Detection of Electromagnetic Emission Transmitted to Earthquake Region) micro-satellite. The DEMETER satellite flew close to the epicenter of the earthquakes many times and operated in burst mode. The waveforms registered in this mode can be analyzed using wavelet, bispectral and statistical methods to detect the ULF-VLF disturbances in the ionospheric plasma. The geomagnetic conditions ($Dst < 50\,nT$) were quiet during a period of two week prior to the earthquakes indicating that the VLF disturbances observed were less likely of magnetospheric origin due the geomagnetic disturbances.

NPGD
1, 977–997, 2014

2 Theoretical framework

Fourier analysis is inappropriate for the analysis of turbulence in the plasma (Farge, 1996); therefore we have used wavelet transform technique. The usefulness of wavelet to detect the turbulence was underlined by Farge (1992) in the context of coherent structures. The main advantage of wavelet transform is that it preserves the information about the local features (e.g. singularities) of the signal and also allows reconstruction of the signal over a given range of scales. This property is of importance in the study of turbulence, which often shows coherent structures that are apparently related to non-linear processes. More discussion about wavelet transform and its applications to turbulence analysis can be found in number of books and review articles (e.g. Farge et al., 1996; Mallat, 1998; Wernik, 2002, 2005). A more detailed description of methods used in this work can be found in Błecki et al. (2007, 2009, and 2012).

2.1 Wavelet power and global wavelet spectrum analysis

Wavelet-based analyses involve the use of the Continuous Wavelet Transform (CWT) (Torrence and Compo, 1998) of VLF transients $f(t)$ sampled at time steps δ_t. For all time indexes n CWT can be calculated as:

$$Wf(x,s) = \sum_{k=0}^{N-1} \hat{f}_k \bar{\hat{\psi}}_s(s\omega_k) e^{i\omega_k n\delta t}, \tag{1}$$

where ($\hat{}$) indicates the Fourier transform, k the frequency index and $\omega_k = \pm\frac{2\pi k}{N\delta t}$ the angular frequency. For convenience, the scales are written as $s_j = 2\delta_j 2^{j\delta_j}$, $j = 0, 1, \ldots, j$.

The scale averaged wavelet power spectrum (WPS) is used to examine fluctuations in signal power over a range of scales. It is obtained by averaging the local wavelet coefficients along the N-vertical cuts of the time axis for a range of scales from s_1 to s_2

NPGD
1, 977–997, 2014

(Markovic and Koch, 2005):

$$\bar{W}_n^2 = \frac{\delta_j \delta_t}{C_\delta} \sum_{j=j_1}^{j=j_2} \frac{|Wf(x,s)|^2}{s_j}, \quad (2)$$

where C_δ is a scale independent characteristics of the basic function used (Torrence and Compo, 1998). The scale-averaged wavelet power can be viewed as a time series of the average variance in a certain band of scales. The average of the wavelet power over all local wavelet spectra along the time axis is the global wavelet power spectrum (Torrence and Compo, 1998):

$$\bar{W}^2(s) = \frac{1}{N} \sum_{n=0}^{N-1} |Wf(x,s)|^2. \quad (3)$$

The wavelet power spectrum and the global wavelet spectrum provide the main fluctuations in power of VLF signals at different scales and over a range of scales at different times.

2.2 Bi-spectral analysis

The fundamental process involves in the development of plasma turbulence and coherent structure is the wave-wave interaction. The classical bi-spectrum is defined as $B(\omega_1,\omega_2) = \langle X(\omega_1)+X(\omega_2)X^*(\omega_1+\omega_2)\rangle$ which measures the degree of phase coupling between the frequency components of observed signal such that $\omega_1 + \omega_2 = \omega_3$ where $\omega_3 < \omega_{\text{Nyquist}}$. The angle brackets denote an ensemble average. It is an indication of quadratic coupling of the modes of the system (Kim and Powers, 1978). The bi-coherence is the normalized amplitude of the bi-spectrum,

$$b^2(\omega_1,\omega_2) = \frac{|B(\omega_1,\omega_2)|^2}{\langle |X(\omega_1)||X(\omega_2)||X^*(\omega_1+\omega_2)|\rangle^2} \quad (4)$$

and takes a value $b^2 \epsilon \{0,1\}$. The bi-coherence has maxima at frequency pairs which are phase related as $\emptyset(\omega_1,\omega_2) = \emptyset(\omega_1) + \emptyset(\omega_2) - \emptyset(\omega_1 + \omega_2) + \emptyset_0$ and is zero in the presence of randomly phased Gaussian noise.

Kim and Powers (1978) first time used this method for the study of plasma process. It allows the nonlinear interaction between the wave modes by computing the bispectrum of the signal. It provides information about the phase coherence. A quantitative measure of the phase coherency can be obtained using the incoherence spectrum. The first use of bi-spectral analysis for space plasma was given by Tanaka et al. (1987). Bi-spectrum analysis was applied in the study of nonlinear processes in the magnetospheric cusp and ionospheric electromagnetic turbulence analysis in ULF range (Błecki et al., 2007, 2012).

2.3 Statistical analysis

The Probability Density Functions (PDFs) have been suggested useful to understand the phenomena that occur in any turbulent system involving hydrodynamic (Ramos et al., 2001; Bolzan et al., 2002) or magnetohydrodynamic flows (Burloga and Vinas, 2004; Bolzan et al., 2005). These functions indicate whether the phenomenon has random character with PDF that is close to Gaussian or it is intermittent and asymmetric indicating turbulence in the system. The useful parameters to study turbulence are skeweness and kurtosis. The skewness (s) is the third moment of the measured physical value normalized by the variance given as

$$s = \frac{\langle (x-X)^3 \rangle}{\langle (x-X)^2 \rangle^{\frac{3}{2}}}, \tag{5}$$

where x is the measured value (in our case, the electric field intensity) and X denotes its mean value. The skewness reveals information about the asymmetry of the PDF. Positive skewness indicates that the PDF has a longer tail for $x - X > 0$ than for $x - X <$

NPGD
1, 977–997, 2014

Precursors of earthquakes in VLF range observed by DEMETER Satellite

D. K. Sondhiya et al.

0. Hence, a positive skewness means that the variable x is more likely to take on large positive values than large negative values.

The s has been used to investigate the transport asymmetry in hydrodynamics turbulence specifically in Convective Boundary Layer (CBL) in atmosphere (Wyngaard and Weil, 1991). In recent years, there are many works demonstrating the importance of the study of the skewness parameter in magnetohydrodynamics turbulence data obtained in laboratory (Antonov et al., 2000) and experimental sites (Burlaga et al., 2002). The kurtosis (or flatness) is the measure of the intermittency. It is defined as the fourth momentum of the measured physical value normalized by the variance

$$K = \frac{\langle (x-X)^4 \rangle}{\langle (x-X)^2 \rangle^2}. \quad (6)$$

A PDF with longer tails will have a larger kurtosis than a PDF with narrower tails. A time series with most measurements clustered around the mean has low kurtosis, a time series dominated by intermittent extreme events has high kurtosis.

3 Results and discussion

For the analysis of coherent structure and phenomena of intermittence VLF signals have been taken form three different orbits of DEMETER satellite associated with three earthquakes. The characteristics of these earthquakes are given in Table 1.

First we have taken the earthquake that occurred on 26 September 2008, at 18:46:19 UT in Carlsberg Ridge Region. It had its epicenter at 3.06° N and 65.43° E. Its depth was 10 km and magnitude was $M = 5.4$. The closest approach of DEMETER satellite to the epicenter was at 04:25:00 UT on 17 September 2008. The wavelet spectrogram of the electric field waveform in the VLF frequency range up to 20 kHz during a burst mode between 04:33:36 and 05:00:308 UT is presented in Fig. 1a. Figure 1b represents the normalized Wavelet Power Spectrum (right panel) using "Morlet" mother wavelet with its global wavelet power spectrum (right panel). The x axis denotes the current time and the y axis denotes the frequencies or periods in the time series; the gray scale bar represents the third dimension of the periodogram, and denotes the energy associated with each frequency or period. It was found that there exists a high power concentration near 0.3×10^{-3} Hz and 0.1×10^{-3} Hz frequency bands.

To test the statistical significance of the global wavelet power spectrum peaks a theoretical red noise spectrum is defined. The AR(1) model is used to simulate this spectrum with autocorrelation factor estimated directly from the signals. After defining the univariate lag-1 auto regressive model, the background spectrum for red noise is multiplied by the 95th percentile value for χ_2^2 to determine the 5 % significance level (95 % confidence level) of the wavelet global spectrum (Torrence and Compo, 1998). The autocorrelation coefficient is calculated as 0.84. It gives a peak at 0.1×10^{-3} Hz frequency band. It is not statistically significant because located outside the cone of influence. It is probably due to generation of highly intense electric field due to earthquake generation process.

The calculation of bispectrum (Fig. 1c) shows a strong interaction at 0–50 Hz band. Figure 1d shows the example of the single spectrum. The slope of this is about −2.47, which corresponds to the Kolmogorov model of the turbulence.

The probability distribution (PDF) curve (Fig. 2a) along with the parameter of the wave distribution as kurtosis and skewness (Fig. 2b) are presented in Fig. 2. It is found that PDF curve shows distortion in relation to a Gaussian distribution. Wave distribution parameter shows strong enhancement at the time of increase wave activity. This shows the intermittent character of the process.

Secondly, we analyzed the VLF signal observed during the earthquake that occurred at Offshore Antofagasta, Chile, on 9 January 2009 with magnitude $M = 5$. Waveform of VLF signal observed during the earthquake is illustrated in Fig. 3a. Its wavelet power spectrum and global wavelet power spectrum is given in Fig. 3b. It shows high power concentration near 0.3×10^{-3} Hz frequency band and also gives statistical significant peak at this level.

NPGD
1, 977–997, 2014

A clear picture of the turbulent cascade is seen in the lower part of bispectrum illustrated in Fig. 3c. The cascade of the energy appears in the figure as an elongated "red island" parallel to the horizontal frequency axis, from 800 Hz up to 4800 Hz. The energy from the lower frequency was transferred to the higher frequency during the development of the turbulence. Figure 3d shows a single spectrum and again the slope of 1.7 indicates the developed Kolmogorov type of the turbulence.

Figure 4a shows the PDF and the distortion of this plot can be seen in relation to a Gaussian distribution. The parameters of the distribution, as kurtosis and skewness are presented in Fig. 4b. Strong enhancements of these moments were seen at the time of the increase in wave activity.

As the third example, we analyzed the waveform of electric field observed by DEMETER satellite (orbit 24664) on 18 February 2009 at 18:28 UT over the Kepulauan (3.839° N, 126.4° S), Talud, Indonesia, during earthquake ($M = 5.2$) and is shown in Fig. 5a. The Spectrogram shown in Fig. 5b indicates emissions in the VLF range upto 20 kHz which appears to be tweeks or short duration whistlers. The straight line around 19.2 kHz seems to be the signal from VTX3 transmitter located at South Vijaynarayanam, India. Figure 5b presents the normalized wavelet power spectrum with its global wavelet power spectrum of observed VLF signal. It is found that there exists a high wavelet power concentration near the frequency range from 0.15 up to 0.03 Hz showing the clear picture of turbulence. That is the region where whistlers are particularly enhanced up to highest frequency. It also shows transfer of energy from the lower frequency to higher frequency range during the development of turbulence. The combination of both positive and negative peaks into a single broad peak represents the non-stationary present near the higher frequency bands, which can be attributed to various plasmasphere effect generated due to earthquake generation process although these signals (tweeks or short whistlers) would have been generated by strong lightning. Plasma waves that can lead to efficient gyroresonant wave particle interactions with energetic electrons include whistler mode chorus waves, plasmaspheric hiss, lightning-generated whistlers, magnetosonic waves and electromagnetic ion cyclotron waves.

The bispectrum for this disturbance is illustrated in Fig. 5c. It indicates a strong significant 3-wave interaction that is clearly seen in the frequency range of 2694 Hz–3456 Hz. Figure 5d shows the example of the single spectrum with a slope of about 1.68, which corresponds to the Kolmogorov model of the turbulence.

The probability distribution function curve along with the parameters of the wave distribution as kurtosis and skewness are presented in Fig. 6, which show strong enhancement of these moments at the time of increased wave activity.

4 Summary

In this work detailed analysis of electromagnetic wave data observed by the DEMETER satellite prior to the three different earthquakes has been presented. Wavelet and Bispectral techniques based analysis shows many significant effect in the ionosphere few days before the earthquake. Large value of kurtosis shows the higher level of intermittence in the VLF signal before earthquake. It is possible to conjecture that the sources of this intermittence are the coherent structures. Large values of the kurtosis have also been estimated in strongly non-Gaussian probability density functions which are consisted with earlier studies (Hussian, 1983; Kinney and Mc William, 1995; Ramos, 2001; Bolzan, 2002, 2005; Hnat et al., 2003). For the better understanding of this behavior skewness parameter has been estimated. In general, the kurtosis and skewness parameters have shown the same behavior according to results of Burgala and Forman, (2002). The enhanced value of skewness is due to the presence of the coherent structures in the transients. The high energy at the large scales of the VLF turbulence due the earthquake preparation process indicated the generation of coherent structures in the VLF signal. The coherent VLF signals propagating in the terrestrial magnetosphere can trigger diffuse and structured emission bursts. As a result of trapping, the gradient becomes sufficiently steep, and then broad band

NPGD
1, 977–997, 2014

wave growth takes place as predicted by established theories (Nunn, 1997; Nunn et al., 2005). The resulting pitch angle diffusion of particles produces a more stable configuration in which the steep gradient is reduced towards that corresponding to the marginally stable distribution (Kennel, 1996; Artemyev et al., 2013). For initially positive gradients in the energetic electron distribution function with respect to parallel velocity, wave growth takes place above the frequency of the causative coherent signal. The theory predicts that the bandwidth of emissions triggered in this way should rapidly increase with time and may reach maximum widths of several hundred Hz (Matthews, 1985).

Acknowledgements. D. K. Sondhiya is thankful to the University Grant Commission, New Delhi (India) for providing financial support through Special Assistance Program (SAP).

References

Antonov, N. V., Lanotte, A., and Mazzino, A.: Persistence of small-scale anisotropies and anomalous scaling in a model of magnetohydrodynamics turbulence, Phys. Rev. E, 61, 6586–6605, doi:10.1103/PhysRevE.61.6586, 2000.

Artemyev, A. V., Orlova, K. G., Mourenas, D., Agapitov, O. V., and Krasnoselskikh, V. V.: Electron pitch-angle diffusion: resonant scattering by waves vs. nonadiabatic effects, Ann. Geophys., 31, 1485–1490, doi:10.5194/angeo-31-1485-2013, 2013.

Błecki, J., Savin, S., Parrot, M., and Wronowski, R.: Nonlinear interactions of the low frequency plasma waves in the middle-altitude polar cusp as observed by Prognoz-8, Interball-1 and cluster satellites, Acta Geophys., 55, 459–468, 2007.

Błecki, J., Parrot, M., and Wronowski, R.: Can the ionospheric plasma turbulence be a precursor of the earthquake?, Results of DEMETER measurements, in: Proceedings of ESA Swarm Science Workshop, 24–26 Potsdam, 2009.

Błecki, J., Kos'ciesza, M., Parrot, M., Savin, S., and Wronowski, R.: Extremely low frequency plasma turbulence recorded by the DEMETER satellite in the ionosphere over the Abruzzi region prior to the 6 April 2009, L'Aquila earthquake, Ann. Geophys.-Italy, 55, 1, doi:10.4401/ag-5356, 2012.

NPGD
1, 977–997, 2014

Precursors of earthquakes in VLF range observed by DEMETER Satellite

D. K. Sondhiya et al.

Title Page
Abstract | Introduction
Conclusions | References
Tables | Figures
◄◄ | ►►
◄ | ►
Back | Close
Full Screen / Esc
Printer-friendly Version
Interactive Discussion

Bolzan, M. J. A., Ramos, F. M., Sá, L. D. A., Rodrigues Neto, C., and Rosa, R. R.: Analysis of fine-scale canopy turbulence within and above an Amazon forest using Tsallis' generalized thermostatistics, J. Geophys. Res., 107, 8063, doi:10.1029/2001JD000378, 2002.

Bolzan, M. J. A., Sahai, Y., Fagundes, P. R., Rosa, R. R., Ramos, F. M., and Abalde, J. R.: Intermitency analysis of geomagnetic storm time-series observed in Brazil, J. Atmos. Sol.-Terr. Phys., 67, 1365–1372, doi:10.1016/j.jastp.2005.06.008, 2005.

Boskova, J., Smilauer, J., Tıska, P., and Kudela, K.: Anomalous behavior of plasma parameters as observed by the intercosmos 24satellite prior to the Iranian earthquake of 20 June 1990, Stud. Geophys. Geod., 38, 213–220, 1994.

Burlaga, L. F. and F.-Viñas. A.: Multi-scale probability distributions of solar wind speed fluctuations at 1 AU described by a generalized Tsallis distribution, Geophys. Res. Lett., 31, L16807, doi:10.1029/2004GL020715, 2004.

Burlaga, L. F., Plunkett, S. P., and St. Cyr, O. C.: Successive CMEs and complex ejecta, J. Geophys. Res., 107, SSH1-3–SSH1-12, doi:10.1029/2001JA00255, 2002.

Farge, M.: Wavelet transforms and their applications to turbulence, Annu. Rev. Fluid Mech., 24, 395–457, 1992.

Farge, M., Evlahan, K., Perrier, N. V., and Goirand, E.: Wavelets and turbulence, in: Special issue on wavelets, Proceedings of the IEEE, edited by: Daubechies, J. and Kovasevic, J., 84, 639–669, 1996.

Frisch, U.: The Legacy of A. N. Kolmogorov, Cambridge University Press, Cambridge, UK, 1995.

Fuzinawa, Y. and Takahashi, K.: Electromagnetic radiations associated with major earthquakes, 105, 249–259, doi:10.1016/S0031-9201(97)00117, 1998.

Hayakawa, M. (Ed.): Atmospheric and Ionospheric Electromagnetic Phenomena Associated with Earthquakes, Terrapub, Tokyo, 1999.

Hayakawa, M., Molchanov, O. A., and NASDA/UEC team: Achievements of NASDA's earthquake remote sensing frontier project, Terrestrial, Atmospheric and Oceanic Sciences, 15, 311–327, 2004.

He, Y. F., Yang, D. M., Chen, H. R., Qian, J. P., Zhu, R. J., and Parrot, M.: SNR changes of VLF radio signals detected onboard the DEMETER satellite and their possible relationship to the Wenchuan earthquake, SCIENCE CHINA Earth Sciences, 52, 754–763, doi:10.1007/s11430-009-0064-5, 2009.

Hnat, B., Chapman, S. C., and Rowlands. G.: Intermitency, scalingand the Fokker–Planck approach to fluctuations of the solar wind bulk plasma parameters as seen by wind, Phys. Rev. E, 67, 056404, doi:10.1103/PhysRevE.67.056404, 2003.
Hussain, A. K. M. F.: Coherent structure-reality and myth, Phys. Fluids, 26, 2816, doi:10.1063/1.864048, 1983.
Karakelian, D., Klemperer, S. L., Fraser-Smith, A. C., and Beroza, G. C.: A transportable system for monitoring ultra low frequency electromagnetic signals associated with earthquakes, Seismol. Res. Lett., 71, 423–436, 2000.
Kennel, C. F. and Petschek, H. E.: Limit on stably trapped particle fluxes, J. Geophys. Res., 71, 1–28, doi:10.1029/JZ071i001p00001, 1966.
Kim, Y. C. and Powers, E. J.: Digital bispectral analysis of self-excited fluctuation spectra, Phys. Fluids, 21, 1452–1453, 1978.
Kinney, R. and McWilliams, J. C.: Coherent structures and turbulent cascades in twodimensional incompressible magnetohydrodynamic turbulence, Phys. Plasmas, 2, 3623–3639, 1995.
Mallat, S. A.: Wavelet Tour of Signal Processing, Academic Press, San Diego, 1998.
Markovic, D., and Koch, M.: Wavelet and scaling analysis of monthly precipitation extremes in Germany in the 20th century: inter annual to inter decadal oscillations and the North Atlantic Oscillation influence, Water Resour. Res., 41, W09420, doi:10.1029/2004WR003843, 2005.
Matthews, J. P.: A theory of diffuse emission bursts triggered by coherent VLF signals propagating parallel to the geomagnetic field, J. Geophys. Res., 90, 2910–2914, 1985.
McComb, W. D.: The Physics of Fluid Turbulence, Clarendon press, Oxford, 1990.
Molchanov, O. A.: On the origin of low- and middlelatitude ionospheric turbulence, Phys. Chem. Earth, 29, 559–567, 2004.
Nagao, T., Enomoto, Y., Fujinawa, Y., Hata, M., Hayakawa, M., Huang, Q., Izutsu, I., Kushida, Y., Maeda, K., Oike, K., Uyeda, S., and Yoshino, T.: Electromagnetic anomalies associated with 1995 KOBE earthquake, J. Geodyn., 33, 401–411, 2002.
Nunn, D., Omura, Y., Matsumoto, H., and Yagitni, N. S.: The numerical simulation of VLF chorus and discrete emissions observed on the Geotail satellite using a Vlasov code, J. Geophys. Res., 102, 27083–27097, 1997.
Nunn, D., Rycroft, M., and Trakhtengerts, V.: A parametric study of the numerical simulations of triggered VLFemissions, Ann. Geophys., 23, 1–12, 2005, http://www.ann-geophys.net/23/1/2005/.

Discussion Paper | Discussion Paper | Discussion Paper | Discussion Paper |

NPGD
1, 977–997, 2014

Precursors of earthquakes in VLF range observed by DEMETER Satellite

D. K. Sondhiya et al.

Pulinets, S. and Boyarchuk, K.: Ionospheric Precursors of Earthquakes, Springer, Berlin, 2004.
Ramos, F. M., Rosa, R. R., Neto, R. R., Bolzan, M. J. A., and S'a L. D. A.: Non-extensive statistics and three-dimensional fully developed turbulence, Physica A, 295, 250–253, 2001.
Sorokin, V. M.: Plasma and electromagnetic effects in the ionosphere related to the dynamics of charged aerosols in the lower atmosphere, R. J. Phys. Chem. B, 1, 138–170, 2007.
Sorokin, V. and Hayakawa, M.: Generation of seismic related DC electric fields and lithosphere–atmosphere-ionosphere coupling, Modern Applied Science, 7, 1–25, doi:10.5539/mas.v7n6p1, 2013.
Tanaka, Y., Lagoutte, D., Hayakawa, M., and Lefeuvre, F.: Spectral broadening of VLF transmitter signalsand sideband structure observed on Aureol-3 satelliteat middle latitudes, J. Geophys. Res., 92, 7551–7559, 1987.
Torrence, C. and Compo, G. P.: A practical guide to wavelet analysis, B. Am. Meteorol. Soc., 79, 61–78, 1998.
Wernik, A. W.: High-latitude ionospheric plasma turbulence: advanced analysis methods and results, Acta Geophysica Polonica, 50, 119–134, 2002.
Wernik, A. W.: Application of the wavelet transform to investigation of space plasma turbulence, in: Proceedings of the International Workshop on Applications of Wavelets to Real World Problems, Istanbul, Turkey, 17–18 July, edited by: Hasan Siddiqi, A., Alsan, S., Rasulov, M., Oguz, O., and Aslan, A., 49–66, 2005.
Wyngaard, J. C. and Weil, J. C.: Transport asymmetry in skewed turbulence, J. C. Phys. Fluids A-Fluid, 3, 155, doi:10.1063/1.857874, 1991.
Zhao, B., Wan, W., Wang, M., Liu, L., and Ninget, B: Recent advances on the ionospheric precursors of earthquakes and ionospheric variation prior to Wenchuan earthquake, Sci. & Technology Rev., 26, 30–34, 2008 (in Chinese with English Abstract).

NPGD
1, 977–997, 2014

Precursors of earthquakes in VLF range observed by DEMETER Satellite

D. K. Sondhiya et al.

Table 1. Characteristics of Earthquakes.

Date	Time	Orbit	Co-ordinate of Epicenter	Depth (km)	M	Region
26 Sep 2008	18:46:19	22514	3.06° N; 65.43° E	10	5.4	Carlsberg Ridge
9 Jan 2009	22:43:31	24084	−23.124° N; −70.665° E	18.4	5	Offshore Antofagasta, Chile
18 Feb 2009	11:44:15	24664	3.839° N; 126.4° E	47	5.2	Kepulauan, Talud, Indonesia

NPGD
1, 977–997, 2014

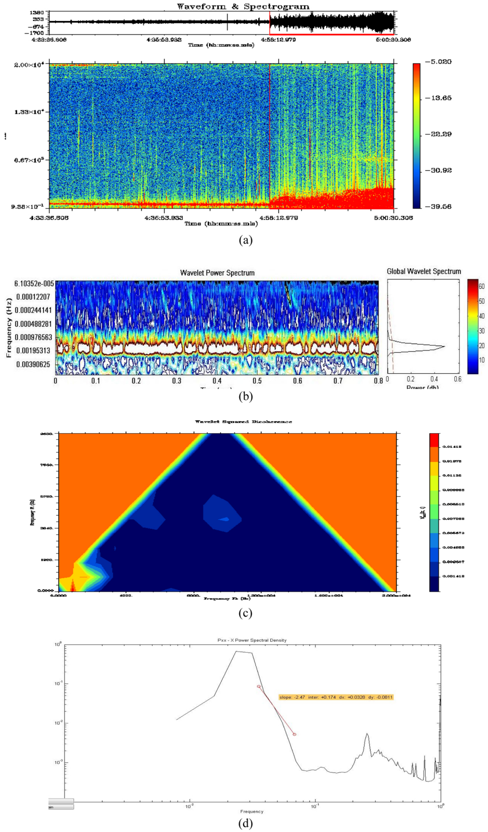

Fig. 1. (a) Waveform and spectrogram of VLF signal (Orbit-22514, Date – 17 September 2008) associated with earthquake – 17 September 2008, M-5.4), **(b)** periodogram and global wavelet transform using Morlet Transform, **(c)** bispectrum of VLF signal, and **(d)** single spectrum with slope ac–2.47.

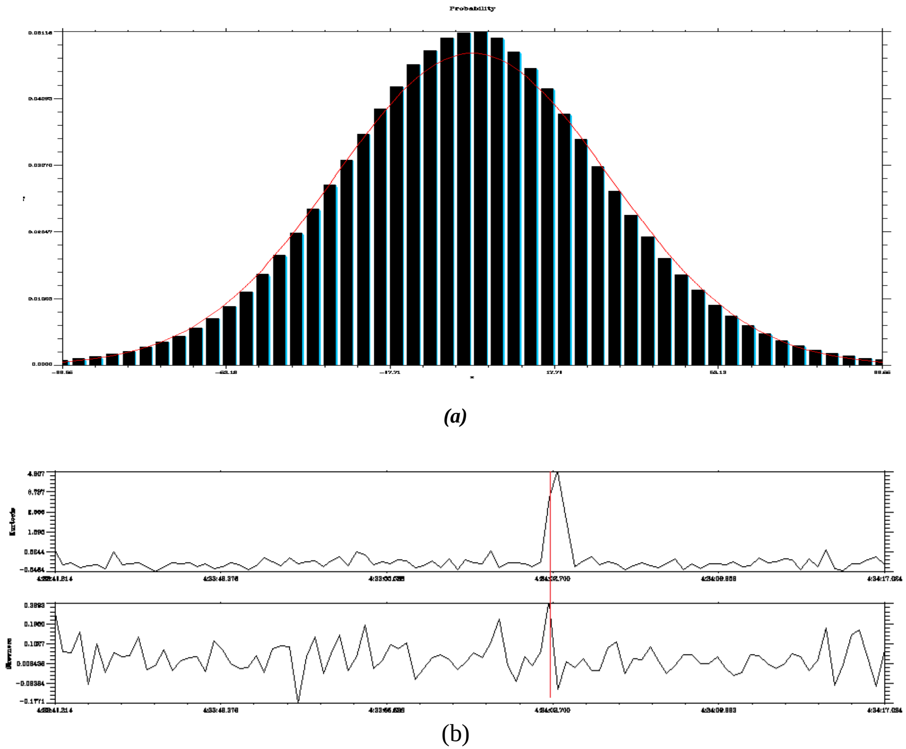

Fig. 2. (a) Probability distribution function, **(b)** moments evolution curves for kurtosis and skweness.

NPGD
1, 977–997, 2014

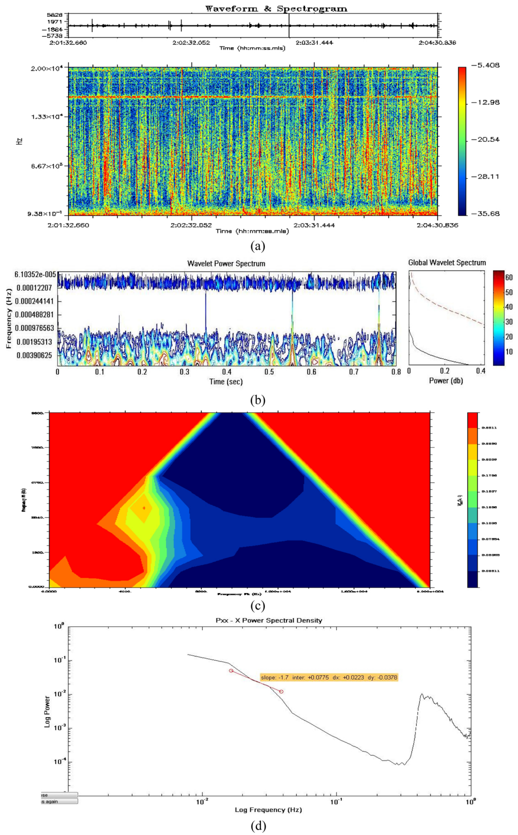

Fig. 3. **(a)** Waveform and spectrogram of in VLF frequency range using SWAN. (Orbit-24084, Date – 18 February 2009, associated earthquake – 18 February 2009, M-5), **(b)** periodogram and global wavelet transform using Morlet Transform, **(c)** bispectrum of VLF signal observed 9 January 2009, and **(d)** single spectrum with slope ac–1.7.

NPGD

1, 977–997, 2014

Precursors of earthquakes in VLF range observed by DEMETER Satellite

D. K. Sondhiya et al.

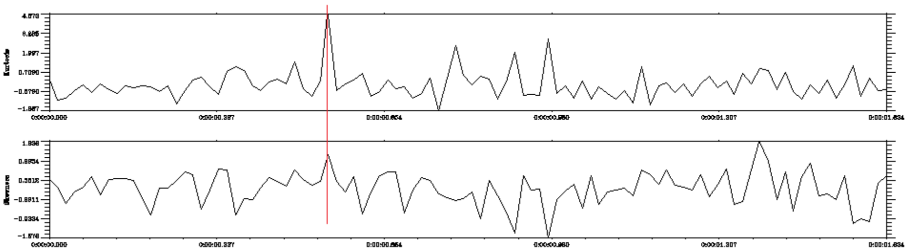

(b)

Fig. 4. **(a)** Probability distribution function, **(b)** moments evolution curves for kurtosis and skweness, 9 January 2009.

NPGD
1, 977–997, 2014

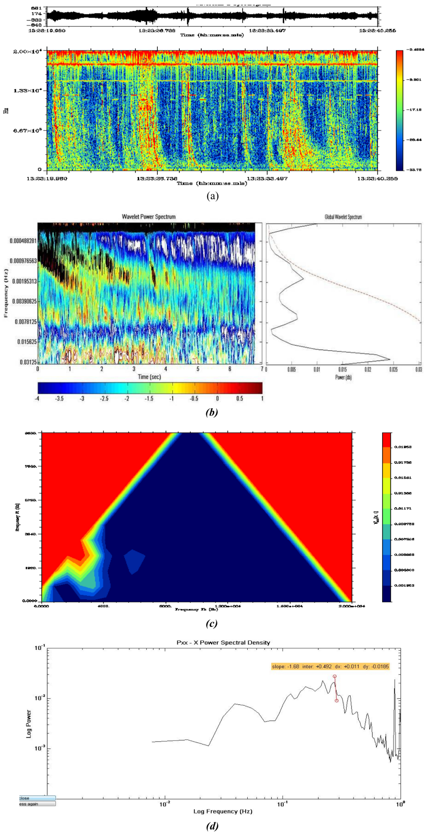

Fig. 5. (a) Waveform and spectrogram of in VLF frequency range using SWAN. (Orbit-24664, Date – 4 February 2009, associated earthquake – 4 February 2009, M-5.2), **(b)** periodogram and global wavelet transform using Morlet Transform, **(c)** bispectrum of VLF signal observed 18 February 2009, and **(d)** single spectrum with slope ac–1.6818.

NPGD
1, 977–997, 2014

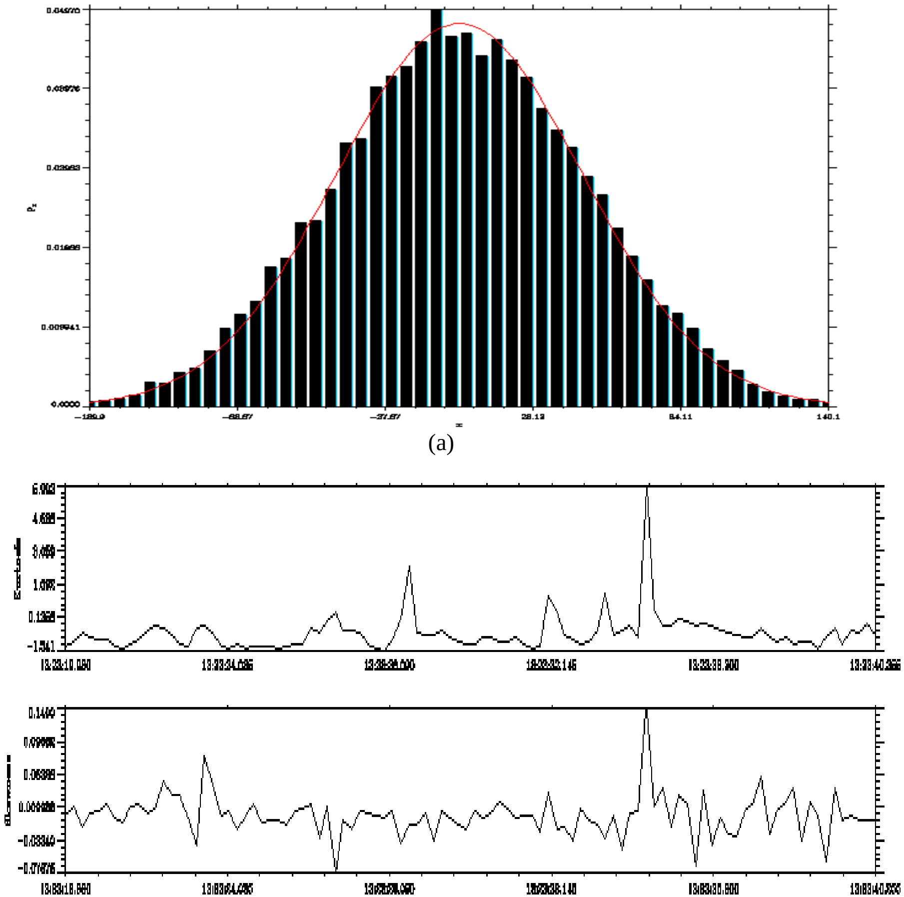

(a) (b)

Fig. 6. (a) Probability distribution function, **(b)** moments evolution curves for kurtosis and skweness, 4 February 2009.